

Introduction

In 1991, Iijima discovered insoluble, nanoscaled, tube-shaped, carbon forms produced by arc burned graphite: carbon nanotubes. Since then, the structural, chemical, and electronic properties of carbon nanotubes have been investigated for the development of new materials and electronic devices.

This report explains work accomplished from fall 2006 through summer 2008 for Dr. Kwon to model nanotube electronic devices. The work was funded in part by the Center for High-Rate Nanomanufacturing (CHN), and collaborative experimental development of nanoscaled devices was done by Dr. Seunghun Hong's group at Seoul National University (SNU) and for nanotube growth by Northeastern University. Although, it was a work in progress, the following peer reviewed papers and American Physics Society March Meeting presentations were accomplished in addition to the required CHN poster presentations during that time period:

- Hahm, Noah, Kwon, Jung, *Diameter Selective Growth of Vertically Aligned Single Walled Carbon Nanotubes by Ethanol Flow Control*, Nanotech 2008 Vol. 1
- Lee, Noah, Park, Seong, Kwon, and Hong, *"Textured" Network Devices: Overcoming Fundamental Limitations of Nanotube/Nanowire Network-Based Devices*, Small (2009)
- Lee, Baik, Noah, Kwon, Lee, and Hong, *Nanowire and Nanotube Transistors for Lab-on-a-Chip Applications*, Lab on a Chip, Issue 16 (2009)
- Noah and Kwon, *Toward 100% Semiconducting Devices From Mixed Chirality Nanotube Networks*, APS (2007)
- Lee, Im, Lee, Myung, Kang, and Hong, *Large-Scale Array of Pristine Carbon Nanotube Transistors*, APS (2007)
- Noah and Kwon, *Modeling Narrow Channel Textured Networks*, APS (2008)
- Lee, Hong, Noah, Kwon, Park, and Seong, *Fabrication of Long Channel Carbon Nanotube Network Transistor Arrays*, APS (2008)
- Park, Lee, Lee, Hong, Kwon, Noah, Park, Seong, *Structural Control of Carbon Nanotube Networks for High-Performance Devices*, APS (2010)

A model of semiconducting channels of random two-dimensional networks of nanotubes was created specifically for evaluation of their applicability to replace field effect transistors and for novel sensor design. Dr. Kwon had intended for this work to be a PhD dissertation, but he had to leave University of Massachusetts, Lowell, at the end of 2008 for personal reasons. Now it is being used 'in lieu' of a master's thesis.

Background About Carbon Nanotubes

Not all readers of this report are familiar with nanotubes, so a brief description is provided here. Carbon nanotubes and spherical buckyballs are members of the fullerene structural group and composed entirely of carbon atoms. The diameter of a nanotube is a few nanometers, but the lengths vary depending on manufacturing conditions. The record to date is something like 18 cm. Single Walled nanotubes (SWNT) can be regarded as a rolled sheet of graphene. Multiwalled nanotubes (MWNT) are concentric cylindrical nanotubes of different diameters. Of particular interest to the development of

sensors, are Double Walled nanotubes (DWNT) since their carbon bonds of the outer wall can break letting them be functionalized.

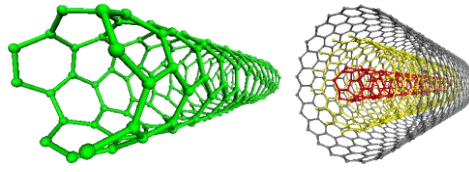


Figure 1: (Left) Single Walled Nanotube (Right) Multiwalled Nanotubes

Graphene is a hexagonal lattice, and the chirality vector:

$$\text{Chirality Vector} = n\vec{a}_1 + m\vec{a}_2$$

is used to describe the connection between points of that lattice when the grapheme is rolled. The basis vectors are shown in Figure 2.

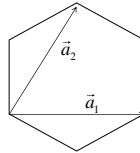


Figure 2: Basis vectors for a hexagonal lattice.

Figure 3 shows the three different ways that grapheme can be rolled to form

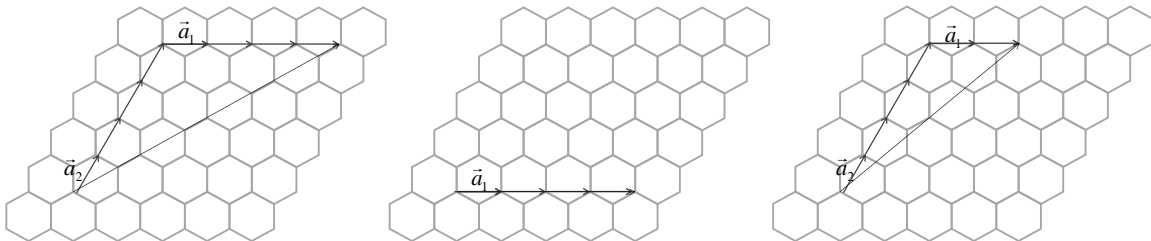
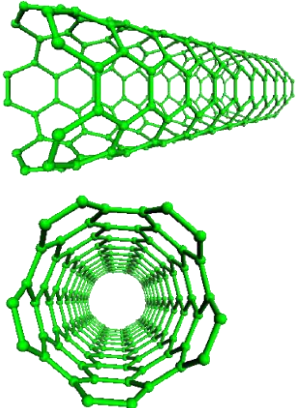
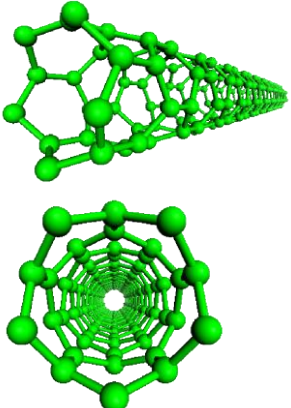
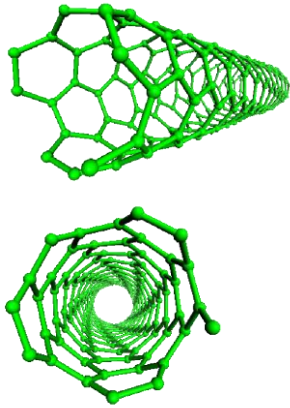


Figure 3: (Left) Armchair Chirality vector $n=m$ (Center) ZigZag Chirality vector $m=0$ (Right) Chiral Chirality vector $n \neq m$

The bonds in CNT are much stronger than in diamond, and yield unique physical and chemical properties. CNT are flexible but extremely strong, about 100 times stronger (stress resistant) than steel yet they are light-weight having 1/6th the mass of steel. CNT are either conductors or semiconductors, and conductors exhibit intrinsic superconductivity (ballistic electron transport). They are ideal thermal conductors and have been used as field emitters. Table 1 gives the electronic properties for different chirality vectors.

Table 1: Chirality and Electronic Properties

	Armchair	ZigZag	Chiral
Lattice vector Relation	$n=m$	$m=0$	$n \neq m$
Fraction Metallic	1	1/3 metallic when $n=3 \times \text{integer}$	1/3 metallic when $(n-m)=3 \times \text{integer}$
Fraction Semiconducting	0	2/3	2/3
Example			
Number of atoms	(5,5) 200 atoms	(5,0) 200 atoms	(5,3) 196 atoms
Diameter	.678 nm	.391 nm	.548 nm
Length	2.460 nm	4.260 nm	2.982 nm
Type	Conductor	Semiconductor	Semiconductor

Metallic SWNT's exhibit ballistic electron transport, that is, they have conductivity that is more like a superconductor than a conductor because the carriers (usually holes unless doped) travel along their length without collision with a carbon atom. Experimental measurements of nanotube conductivity done in 1998 by Stephan Frank showed that nanotubes are ballistic conductors with quantum behavior: the conductance of MWNT jumped by increments of $G_0=2e^2/h = 1/12.9 \text{ k}\Omega^{-1}$. In 1999, Sanvito, Kwon, Tomanek, and Lambert calculated the ballistic quantum conductance of MWNTs and were able to explain Frank's experimental results. Thess (1996) measured the resistivity of ropes of metallic SWNTs to be $10^{-4} \Omega\text{-cm}$ at 300K; and Frank (1998) measured current densities exceeding 10^7 A/cm^2 . According to Hong (2007), theoretical values of current density exceed 10^9 A/cm^2 and that is 1000x higher than copper.

Identification of the Opportunity

The study of semiconducting channels of random two-dimensional networks of nanotubes is an area of current experimental investigation. These thin films exhibit enhanced electronic properties, and are candidates to replace current silicon-based devices. For example, researchers at Naval Research Laboratory have successfully fabricated SWNTs array on a polymeric substrate with field-effect mobility of $150 \text{ cm}^2/\text{Vs}$, normalized transconductance of 0.5 mS/mm , ratio of on current I_{on} to off current I_{off} of about 100 (Snow, 2005). These devices are limited by the presence of metallic SWNTs.

Theoretical models are needed to determine which processes are cost-effective for volume production. No theoretical foundation for nanocomposite network thin-film transistors comparable to Shockley's theory of classical transistors currently exists. Our motivation is to contribute to the development of such a comparable theory for nanoscaled transistors.

Isotropic percolating stick models predict manufacturing difficulties in the development of cost-effective mass production processes. The modeling community has not yet produced a first principles model for understanding both the scaling behavior of the degree of anisotropy in a channel and for predicting the electronic properties of a channel as a function of the degree of anisotropy. Our percolating stick model uses ab initio and measured computations of the electronic properties of individual SWNT to predict properties of ensembles of networks using Monte Carlo simulations.

In 2007, Dr. Hong's group at Seoul National University published their innovative approach to mass production of high-performance flexible electronics involving a scalable strategy for creating high-density arrays of aligned nanotubes. SNU used this method to create field effect transistors with carbon nanotube network channels. Their innovation is revolutionary for several reasons:

- 1) Since the networks are anisotropic or 'textured', they are scalable.
- 2) Their process uses equipment that is readily accessible manufacturing equipment already in place in the semiconductor industry.
- 3) Their process doesn't require separating metallic and semiconducting nanotubes.

The take-home message is that both experimental and simulation results showed that the conductivity and mobility of anisotropic network devices increased with reduced channel width, unlike isotropic networks or conventional silicon devices.

The model was further developed to predict CNT network response to environmental conditions. This will enable experimentalists to determine what environmental factors are significant for performance. It will also allow for the conceptual design of chemical, gas, and pressure sensors.

Isotropic Percolating Stick Models

An isotropic dispersion of nanotubes can be modeled as a two-dimensional field of percolating sticks. Percolation theory describes the formation of long range connectivity in random systems. Two aspects that are important to percolation theory, regardless of the size and shape of connected objects that form a path are 1) the percolation threshold is the minimum density of connecting entities that provide connectivity and 2) the scaling behavior is the description of how that threshold depends on the dimensions of connected entities.

Computational percolating stick models were first pursued in the 1970s for better understanding oil flow through fissures in rocks. Fractal and percolation theories show that an infinitely large network of sticks will percolate at a threshold density that is inversely proportional to the square of the stick length. Pike and Seager (1974) derived this relation using a Monte Carlo computer model:

$$\rho_{th} = \frac{4.26^2}{\pi L_{Stick}^2}$$

Balberg, Binenbaum, and Anderson (1983) modeled a network of resistors as a percolation of conducting sticks. They defined the critical stick length $L_{Critical}$ for given density of sticks to percolate between two opposite boundaries of a square network. They studied the scaling behavior of the ratio of stick length to that critical stick length and found a conductivity exponent of $t=1.24 \pm 0.03$:

$$\left(\frac{L_{Stick}}{L_{Critical}} \right)^2 - 1 = 10^{1.24}$$

For their work, they developed an anisotropy metric, but used it to exclude networks from the Monte Carlo simulation to be certain that the networks were very isotropic.

Over the past decade, researchers have been applying isotropic percolating sticks to model the conductivity of nanotubes networks. These models evaluate the scaling behavior of conductivity, σ , to the dimensions of a field effect transistor where:

L_{Stick} = the length of a nanotube in the channel

$L_{ChannelLength}$ = the distance between the source and the drain electrode

$L_{ChannelWidth}$ = the length of the intersection between the channel
and the source (or drain) electrode

Pimparker, Guo, Alam (2006) studied the scaling behavior of conductivity and channel length for isotropic systems, and found relations between source-drain current and stick length. They found that conductivity is a power of channel length:

$$\sigma \sim L_{ChannelLength}^\beta$$

Hecht, Hu, Grüner (2006) showed that conductivity is a power law of nanotube stick length:

$$\sigma \sim L_{Stick}^\alpha$$

Finally, and most significantly, Behnam, et al (2006) showed that conductivity is a power law of channel width:

$$\sigma \sim L_{ChannelWidth}^\gamma$$

Figure 4 shows the manufacturing limitation predicted by isotropic stick models: the conductivity decreases with decreasing channel width.

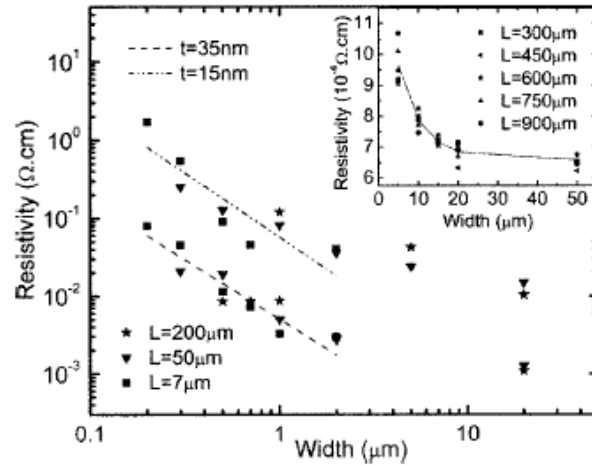


Figure 4: From Behnam, et al (2006). A problem for manufacturing is that resistivity increases as channel width decreases.

SNU Approach to High-Rate Nanomanufacturing of Nanotube Field-Effect Transistors

For SNU's fabrication process, described in this section, the nanotubes dispersed near the edges of the channel rotate to align with the edge rather than cross it. When the channel width is large compared to the nanotube stick length, networks are isotropic. Even though there is some degree of alignment with the edge the channel itself is quite large compared to the area regarded as the edge. But when the channel widths are small, the nanotubes rotate into textured patterns and orient themselves along the channel. Figure 5 is a schematic of the processing steps, and illustrates these two possibilities.

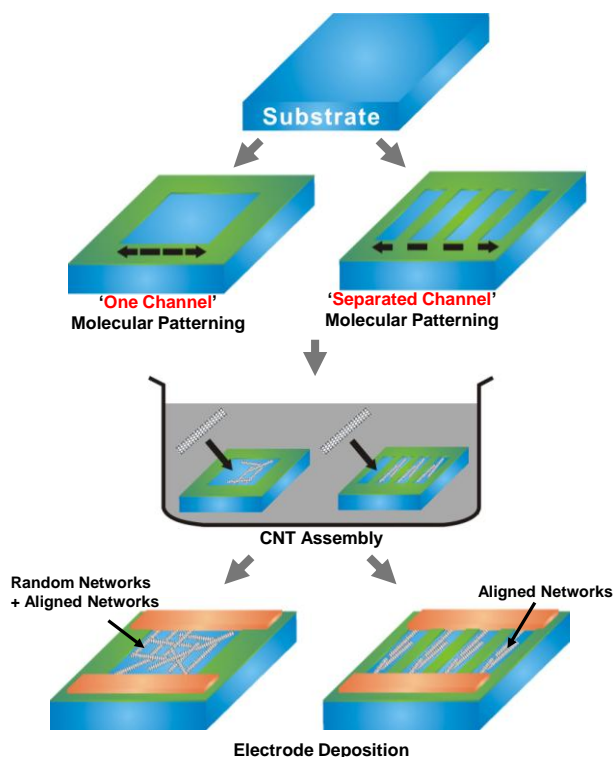


Figure 5: Schematic of Fabrication Procedure. (Left) Isotropic network. (Right) Anisotropic network.

The following description of the processing is from private communication with Minbaek Lee and SNU's contributions to the article in Small (2009). The processing steps are also outlined in Table 2 with figures from Minbaek Lee.

The surface molecular patterning process uses photoresist (AZ1512) for micrometer-sized surface patterns and e-beam resist (ma-N 2401) for nanometer-sized surface patterns. These are patterned onto thermally SiO₂ (1000Å) grown silicon substrates. To pattern a self-assembled monolayer with non-polar terminal groups onto SiO₂ surfaces, octadecyltrichlorosilane is used. The photoresist (or e-beam resist) patterned substrates were dipped in the octadecyltrichlorosilane solution (1:500 (v/v) in anhydrous hexane) for 100 to 200 s. To prevent octadecyltrichlorosilane aggregation, the substrates were immediately cleaned by rinsing with anhydrous hexane, and the photoresist (or e-beam resist) removed with acetone.

Carbon Nanotechnologies manufactured the purified SWNT suspensions used to populate the channels. These are grown from a HiPCO method and have an average length of about 650 nm. Here the mixed chirality CNT sonicated in o-dichlorobenzene (0.1 mg/mL) are selectively adsorbed onto the bare SiO₂ regions up to a full monolayer (the process is self-limiting). The suspensions were sonicated for 20 minutes prior to having the patterned substrate surfaces placed into the solution. To obtain various effective network densities, different concentrations of SWNT solution and dipping periods of the substrate were utilized. After SWNT assembly, a typical lift-off process was employed to fabricate metal contact electrodes of Pd, 20nm in thickness. The back-gate bias voltage was applied through a 100 nm thick SiO₂ layer to measure transistor behaviors. The electrical characteristics of SWNT network devices

were obtained by using a semiconductor characterization system (model: 4200-SCS, Keithley Instruments, Inc.).

Table 2: Outline of SNU Textured Network Fabrication Procedure.

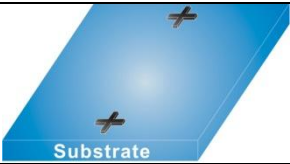
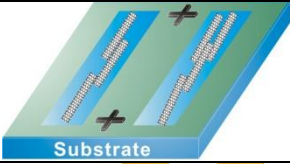
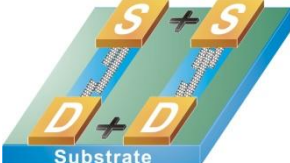
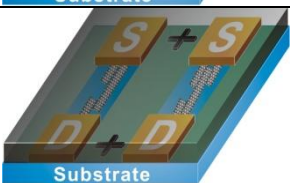

1. Pattern an Alignment Key onto a substrate.	
2. Assemble the CNT onto the substrate.	
3. Pattern the electrodes onto the CNT channels.	
4. Deposit a SiO ₂ film over the electrodes, CNT channel, and substrate.	
5. Pattern on the Gate after selective burning Back-Gate.	

Figure 6 is an SEM image of a single device channel fabricated by SNU. The channel is 32.7 microns wide and since the nanotubes have an average length of 650 nm the distribution of orientations is isotropic. The I-V characteristics are in the plot to the right of the SEM image. Figure 7 is an SEM image of another single device channel. This channel is 2.5 microns wide so the lensing effect of nanotubes rotating to align with the active part of the patterning is evident. This channel has an anisotropic dispersion. The I-V characteristics of a single 2.5 micron channel are to the right of that image. SNU envisions that a single device be comprised of a set of parallel narrow channels, and the I-V characteristics of 4 2.5 micron channels is plotted to the far right. These were early achievements in the SNU process development and were created by dipping the octadecyltrichlorosilane into a 0.01 mg/ml SWNT suspension for 1 second.

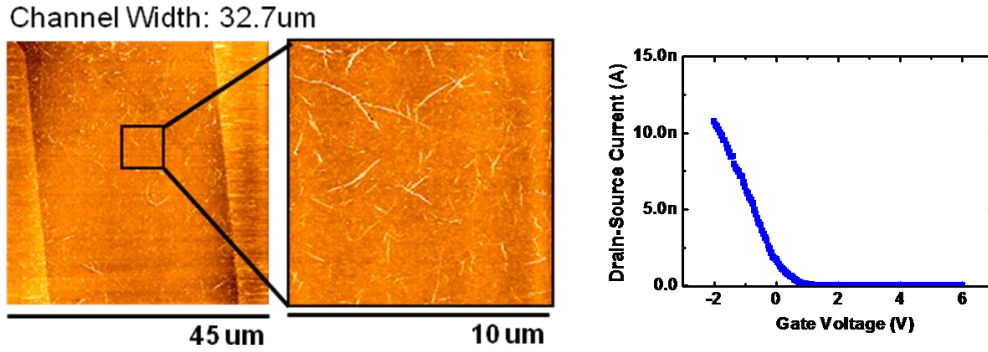


Figure 6: SEM image of a fabricated channel. The nanotubes are averaging 650 nm in length, so this channel is quite wide compared to that length and the dispersion is isotropic. The I-V characteristics are on the right.

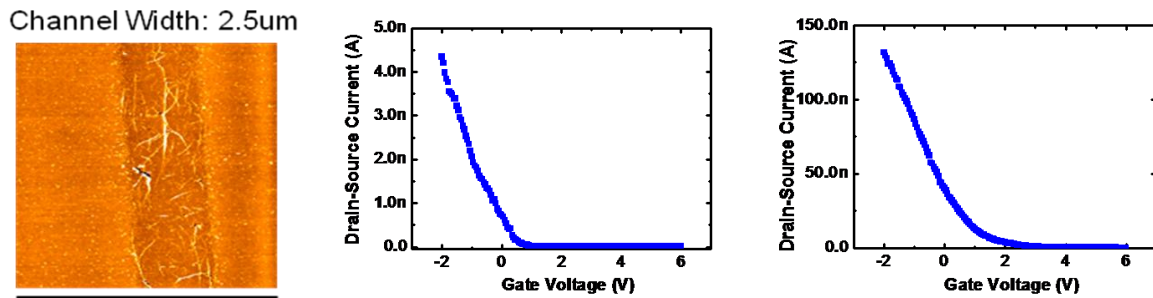


Figure 7: (Left) The channel width is much narrower, so this channel is anisotropic. (Middle) The I-V characteristics of one such channel. (Right) The I-V characteristics of 16 2.5 micron channels as a single device.

Objectives and Methodology

Reiterating from previous sections, our objectives are:

- To model electronic properties of anisotropic nanotube networks.
- To determine the feasibility of using mixed chirality nanotubes.
- To model ensembles of nanotube networks from a statistical characterization of a nanotube mixture.
- To extend the nanotube field effect model to also model sensor s.

Our methodology is to:

- Represent a device as a two-dimensional random network of given length and density dispersed in a channel of given length and width.
- Represent the system as a network of nodes and resistors.
- Reduce the resistor grid using Kirchhoff's Laws.
- Compute resistance of the device.
- Develop a taxonomy of possible outcomes.

- Model ensembles of such devices is created for Monte Carlo simulations.
- From these ensembles, model the distribution functions of each class as a function of nanotube density, length, or channel dimensions.

The output of the model is used to:

- Derive an analytical expression to estimate the probability of success for a give manufacturing parameter set.
- Model the conductivity scaling behavior of isotropic and anisotropic networks.
- Model electronic properties of these devices in different environmental conditions.

The next sections provide the details of this model and the validation against other model output and experimental data.

Modeling Probability of Success in Creating a Semiconducting Channel

To bridge the gap between experimentalists creating one or two semiconductor devices and a processing facility manufacturing millions, a few theoretical questions need to be answered:

1. Can semiconducting devices be created from ensembles of mixed chirality carbon nanotubes, which are readily available to industry?
2. What manufacturing parameters (channel dimensions and nanotube properties) result in the highest number of semiconducting devices?

Modeling the nanotube networks as random fields of percolating sticks, we used a Monte Carlo technique to predict manufacturing success rates given semiconductor design and processing constraints. This model was compared to percolation theory and an analytical expression was developed. The purpose of developing this model is to assist experimentalists and to stream-line and optimize nanomanufacturing.

Figure 8a shows a bird's eye view of a mixed chirality network. We regard it as a system of percolating sticks. Here the red sticks represent metallic nanotubes and the blue sticks represent semiconducting nanotubes. The overlay shows possible subregions that would result from such dispersion on a rectangular template to be the channel between two electrodes in a field effect transistor. If the system were infinite in extent, Pike and Seager predict that percolation would occur when the density of nanotubes is about 0.64 nanotubes per square micron for a random dispersion of 3 micron sticks.

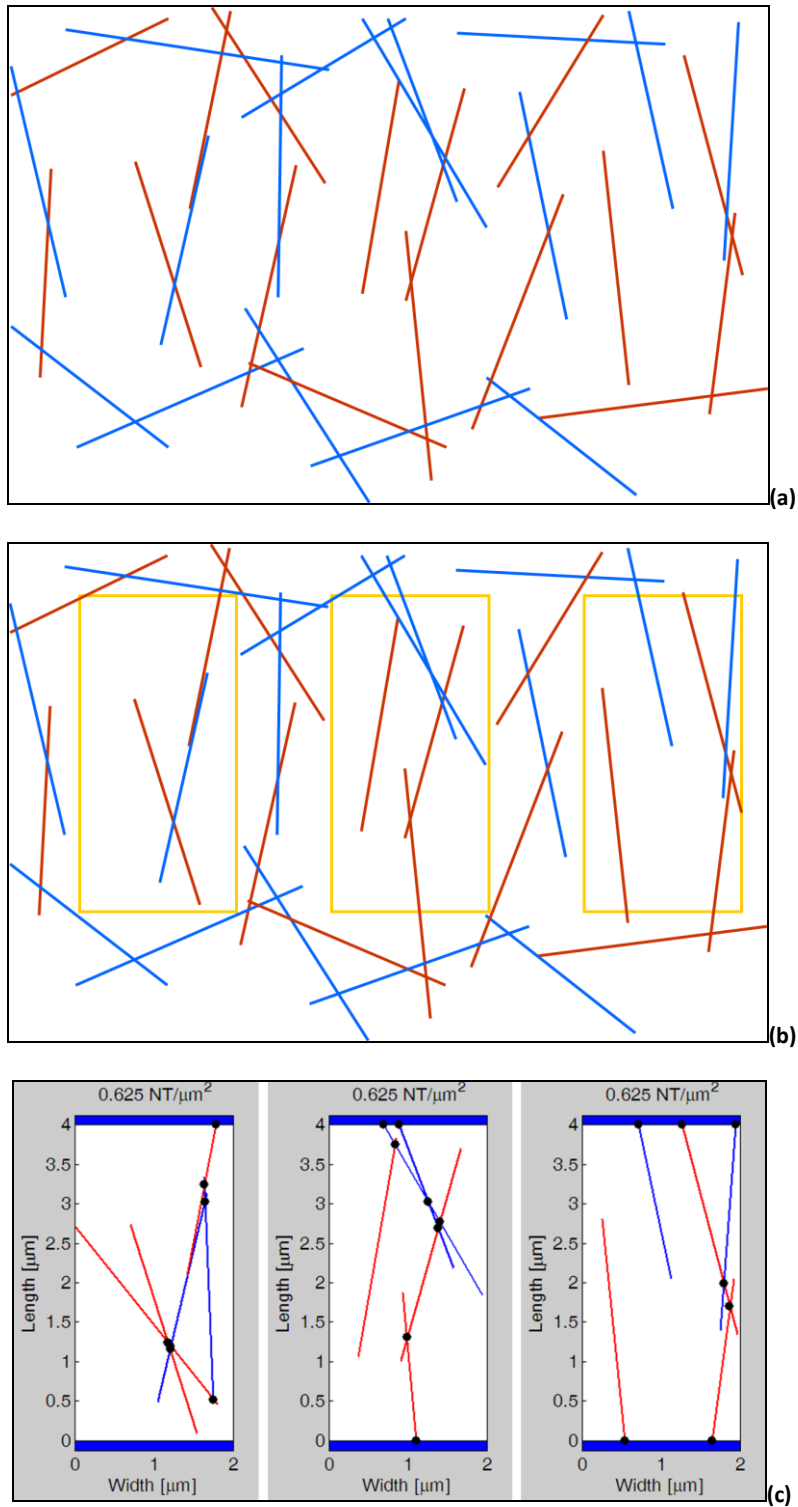


Figure 8: (a) A two-dimensional 'infinite' field of semiconducting (blue) and metallic (red) nanotubes. (b) Possible channel subregions of that random field. (c) Three outcomes for channel properties: left is an insulating channel since there is no path between the electrodes; middle is a semiconducting channel since every path has at least one semiconducting nanotube; right is a metallic channel since there exists a path between the electrodes that is comprised entirely of metallic nanotubes.

As shown in Figure 8b, the channels aren't infinite in extent, and local regions have three possible connectivity classes. These device classes are shown in figure 8c. The first possibility is that the connectivity is broken, so that the device lacks a conducting path from electrode to electrode. If all the tubes are semiconducting, high densities would solve this problem. But with mixed chirality, a high density will result in a device with metallic properties. For an infinite extent channel, when the metallic fraction of tubes is 0.64 nanotubes per square micron, then the device will be metallic. The second possibility for a finite channel is to have a conducting path from electrode to electrode that consists exclusively of metallic tubes. The broken connectivity and the metallic connectivity are undesired outcomes. What industry seeks are techniques for creating semiconducting channels of nanotube networks. The third possible outcome is a channel with at least one semiconducting nanotube along each path of nanotubes connecting the two electrodes. Thus there are three possible classes of devices: not connected, metallic, and semiconducting. Our percolating sticks model can be used to predict the likelihood of each class for a given set of processing parameters.

Our computational approach to model devices is to model the devices as a random dispersion of mixed chirality nanotubes. The dispersion can be modeled with fractal diffusion taking into account the lensing effect of the substrate template which imposes alignment of the nanotubes at the channel edges. The Monte Carlo approach is to statistically characterize outcomes and show the optimal channel dimensions and nanotube density for resulting in the modest semiconducting devices through ensemble statistics. A conceptual block diagram of our model is provided in Figure 9. The inputs to the model are the channel dimensions, the fraction of metallic nanotubes, and nanotube density. These parameters are used to describe a single channel. Another model input is the number of trials for the Monte Carlo statistics.

Figure 9 shows that I-V curves are computed by the model. In this section only the connectivity output is considered, and the computation of I-V curves is discussed in the next section because the original code used a lot of transformations for resistors in parallel, series and the Delta-Y transformation to reduce the grid to a minimum number of resistors then applied Kirchhoff's Laws to find the I-V curves, but after a rewrite WinSpice was used on the table of nodes and resistors without reduction.

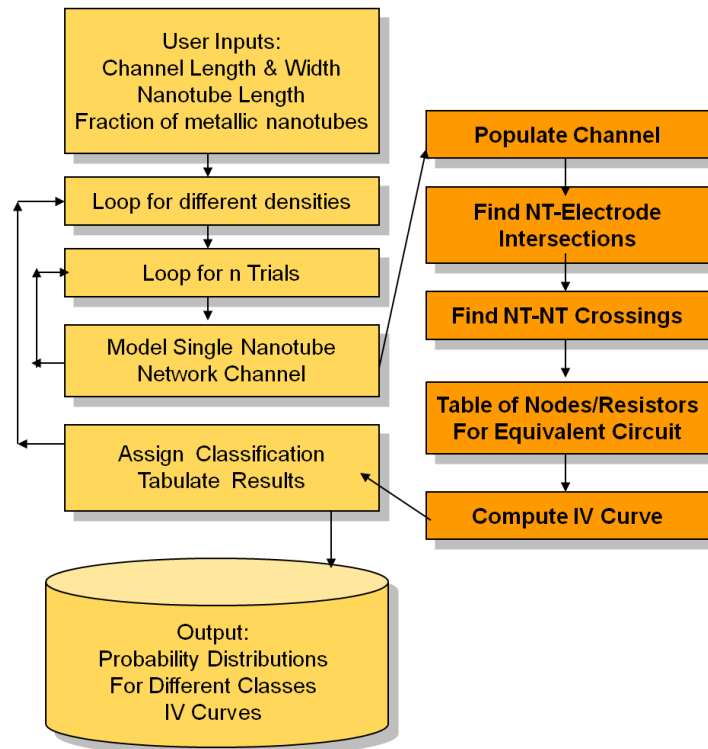


Figure 9: Block Diagram of the Program.

First a channel is modeled by populating it with nanotubes. Internally, the location of the nanotube center, the orientation (angle), and the chirality classification of each nanotube is maintained in a list. Next the locations where nanotubes contact the electrodes and the nanotube junctions in the channel are found. These locations are used to determine the paths of nanotube to junction to nanotube that connect the two electrodes. These paths are assessed to determine their class as semiconducting (at least one semiconducting nanotube) or metallic (all nanotubes along the path are metallic).

Figure 10 depicts the sequence of grid reduction steps from left to right. First the channel is populated with nanotubes. In keeping with the anisotropic model, nanotubes are randomly placed by center and then a random rotation angle is found based on that position so that the entire straight nanotube fits in the channel. Then the points where nanotubes intersect an electrode are found. The next picture shows that the nanotube junctions are found. The next picture shows that the nanotubes are segmented to lengths between junctions. Finally, the segments of nanotubes that start on an an electrode or a junction and terminate in the channel are removed since they do not contribute to the connectivity of the channel.

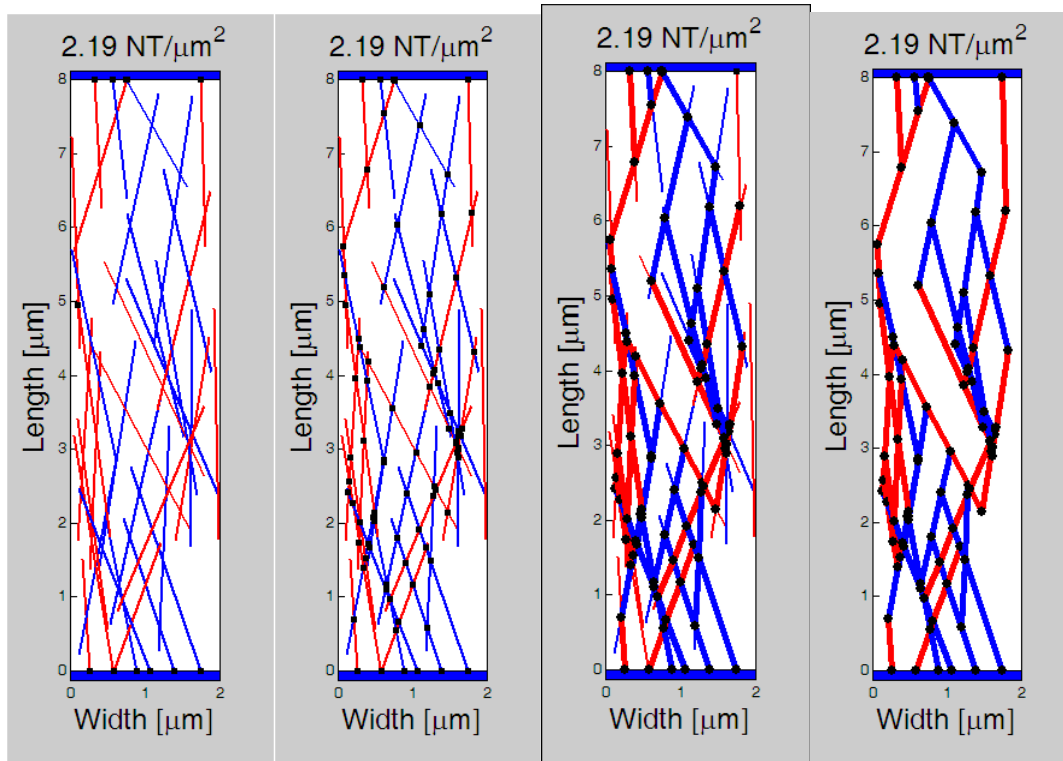


Figure 10: From left to right, these images show the processing steps of reducing the channel nanotube network to a network of resistors.

In this model, the manufacture of semiconducting channels of random two-dimensional networks of nanotubes yields three possible outcomes in terms of connectivity:

1. Success: The device is a semiconductor having a connected path between electrodes that does not have a connected path exclusively comprised of metallic nanotubes.
2. Failure: The device is an insulator, not having a connected path between the electrodes.
3. Failure: The device is a conductor, having a connected path between electrodes of metallic nanotubes.

The model outputs the probability distribution for each class of device.

The probability distribution as a function of nanotube density are shown in Figure 11. The blue line represents the percentage of semiconducting nanotube networks at each density. Manufacturers want a high probability of semiconducting nanotubes and processing parameters that are not too sensitive to variation. For example, statistical ideally won't change significantly as the width or length or density changes.

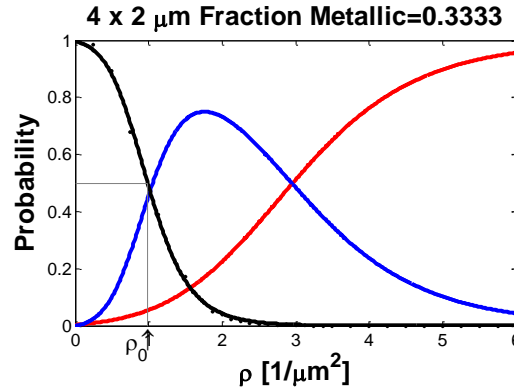


Figure 11: Probability Distributions for an ensemble of 1000 devices that are 4 microns in length and 2 microns in width. The fraction of metallic nanotubes is 1/3. The average nanotube length is 3 microns. The black line shows the probability that a channel is not connected. The red line shows the probability that a channel is metallic. The blue line shows the probability that a channel is semiconducting. A manufacturing facility could never be cost effective with such a low probability of success.

The probability distribution of unconnected networks resembles the Fermi-Dirac distribution function starting with 100% not connecting at low densities, and having a nearly linear slope near the 50% not connecting density, and ending with 100% connecting. In percolation theory, the percolation threshold characterizes the criteria at which a system will percolate. But this applies generally to systems that are infinite in extent. It is inconvenient to use a percolation threshold to characterize systems of percolating sticks that are directional and for a network that is finite in extent.

While percolation threshold is used to describe infinite systems, a more convenient metric for characterizing connectivity in finite systems is the reference point ρ_0 at which 50% of the channels percolate.

The first 'what if' analysis done was to consider how channel length (the distance between the source and drain electrode) affected the outcomes. Figure 12 shows the output when varying the Channel Length from 4 to 180 microns, while holding the channel width at 2 microns, and nanotubes that average 3 microns in length and are of mixed chirality of 1/3 metallic. For these probability distribution plots, 10,000 devices were modeled for an array of densities between 1 and 6 nanotubes per square micron.

When the channel width is held constant, that ρ_0 point occurs at higher densities as the channel length is increased. Here at a channel length of 40 μm , over 90% of devices are connected for a range of densities, the width of densities yielding good statistics as the channel length increases.

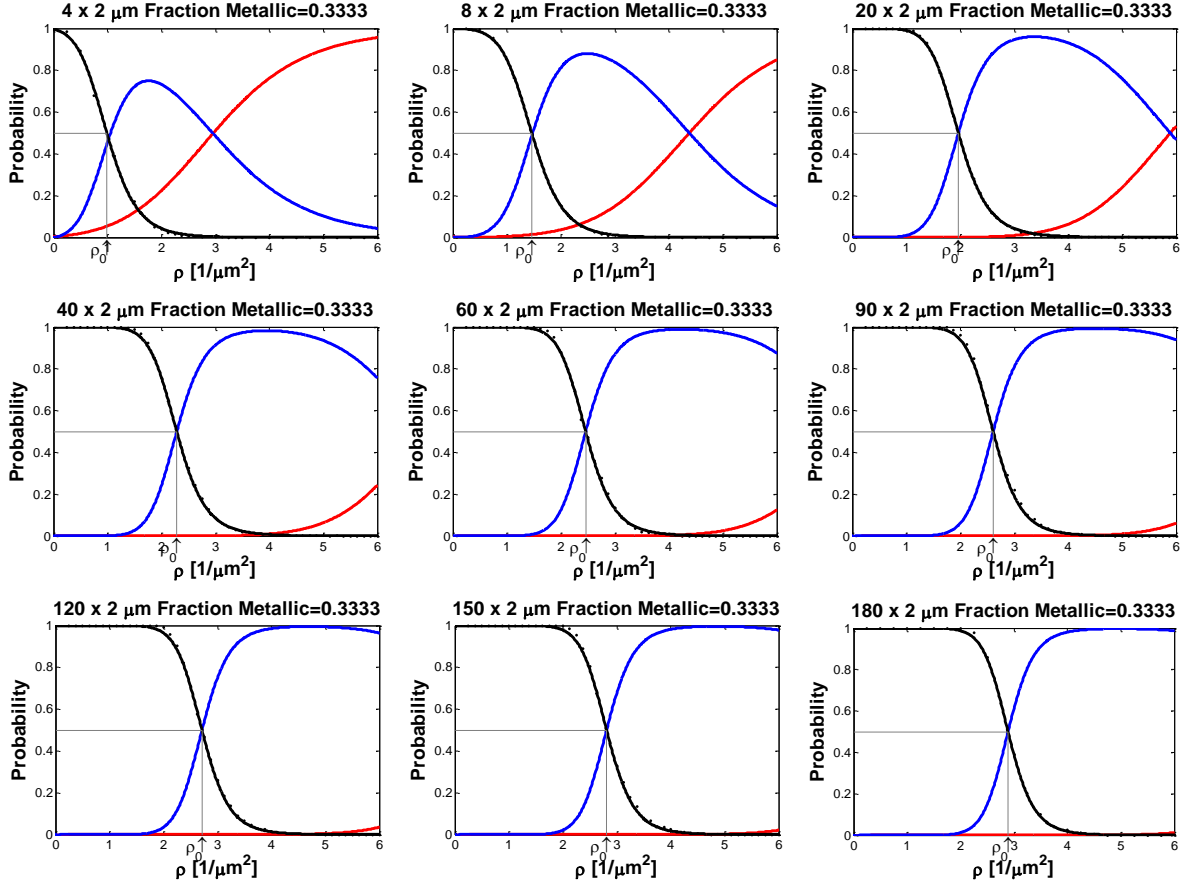


Figure 12: Varying the Channel Length (distance between source and drain electrodes) while holding the channel width at 2 microns, and the fraction of metallic nanotubes at 1/3 and their average length was 3 microns. 10,000 devices were modeled for an array densities between 1 and 6 nanotubes per square micron to find the probability distributions.

While other models focus exclusively on the scaling behavior of conductivity, our model predicts probability of success for a particular channel dimension. If a manufacturer could only turn a profit when there is a probability of success higher than 99%, then for 2 micron wide channels, the length needs to be at least 40 microns. Above that channel length, the probability of success becomes increasingly less dependent on nanotube density, but the minimum density for connection is about 4 nanotubes per square micron.

The second ‘what if’ analysis looked at the affect of varying channel length. Benham’s result showed that conductivity decreases as channel width decreases, and in the next sections it is shown that anisotropic networks give the opposite outcome. But what about the probability of getting a defective channel as width decreases? Using the same nanotube mix as the previous analysis, channel length is held at 20 microns while channel width was varied from 1 to 16 microns. Figure 13 shows that the probability of success increases as the width increases, but it is at a trade-off of sensitivity to density.

When the channel length is held constant, ρ_0 occurs at a lower density as width increases. This result is counter intuitive at first glance, when considering percolation as a function of area. But the channel

connectivity imposes a directional connectivity. Consider two channels side by side. The probability for both of the two channels being unconnected follows the product rule, thus 75% will have at least one of the two channels connecting a single channel ρ_0 density point. Thus doubling the channel width substantially increases the number of connecting devices.

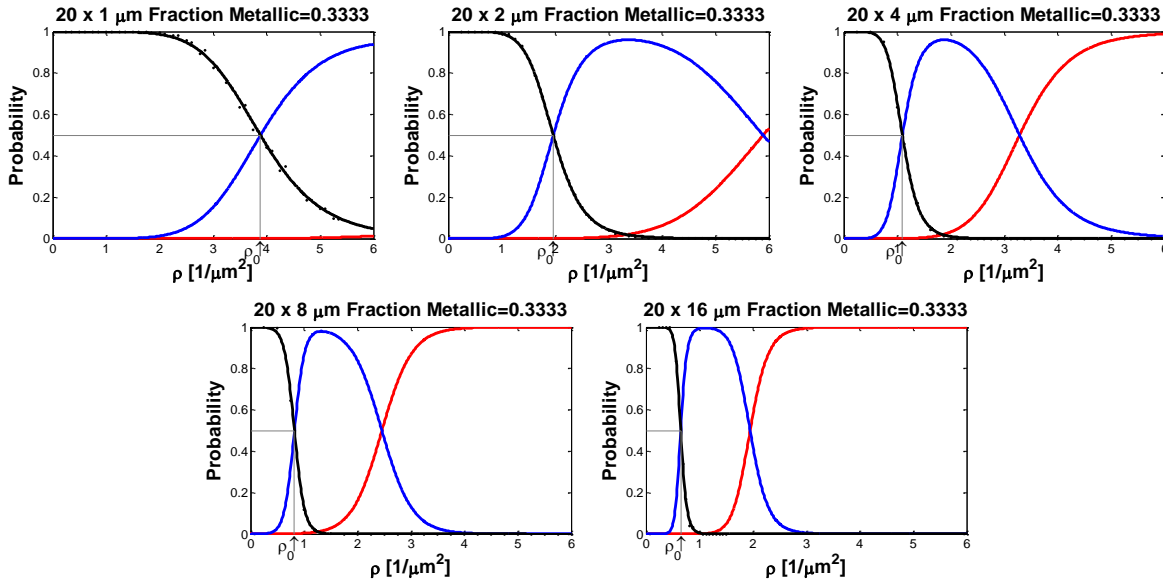


Figure 13: Using the same nanotube mix as the previous analysis, with channel length (distance between electrodes) held at 20 microns, the channel length was varied from 1 to 16 microns. Here the probability of success increases as the width increases, but it is at a trade-off of sensitivity to density.

The final ‘what if’ analysis for our initial model looked at outcomes for changes in the chirality mixture, varying the fraction of nanotubes that are metallic. Figure 14 illustrates the sensitivity to small changes in chirality mix. Even a small change in the fraction of metallic content can result in significantly more or less metallic devices.

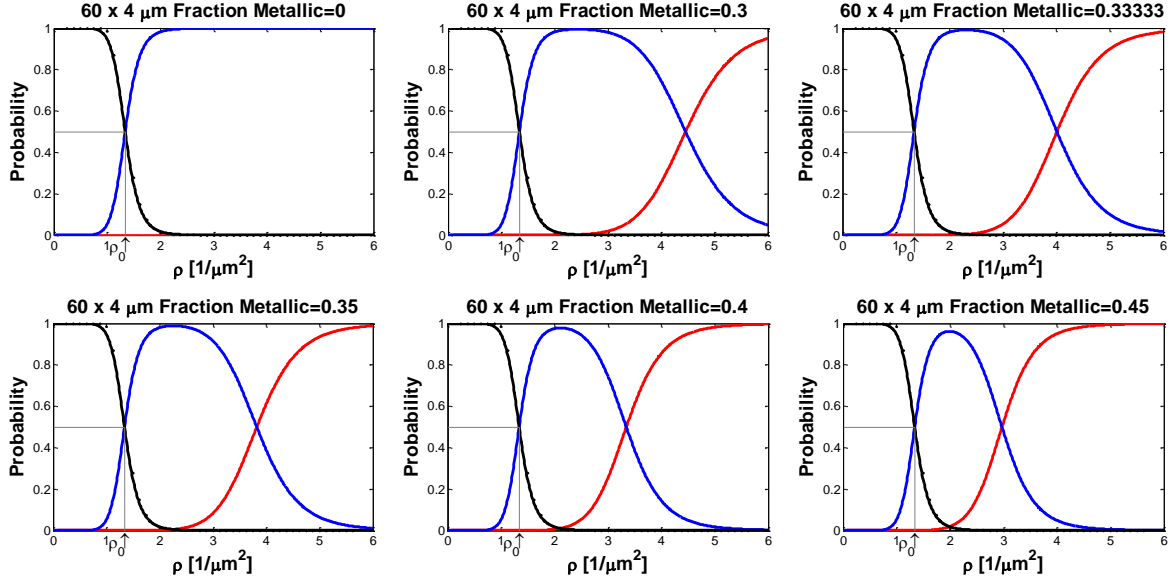


Figure 14: The probability of success is very sensitive to the fraction of metallic nanotubes. Here for a channel length of 60 microns and a channel width of 4 microns, the probability of success exceeds 90% for nanotubes with a 3 micron average length in a mixed chirality where the fraction of metallic nanotubes is varied from 0 to 45%. However, the range of densities that yield a successful outcome decreases with increasing metallic content.

From the model output, an analytical model was developed to predict the probability of success for given the manufacturing parameters of channel dimensions, characteristics of the nanotube mixture, and density of nanotubes in the channel. The following analytical expression was found by fitting the probability curves as a function of density for various nanotube mixtures and channel dimensions:

$$P_{NC}(\rho) = \frac{1}{2} \left\{ 1 - \tanh \left[\beta A^\gamma (\rho^\mu - \rho_0^\mu) \right] \right\}$$

$$P_C(\rho) = 1 - P_{NC}(\rho)$$

$$P_M(\rho) = P_C(f\rho)$$

$$P_{SC}(\rho) = P_C(\rho) - P_M(\rho)$$

$$\rho_0 = f(L, W) = \text{density at which 50\% of devices are connected}$$

$$\mu = \text{asymmetry factor} = 0.0404$$

$$\gamma = \text{slope factor} = 0.2848$$

$$\beta = \text{scaling factor} = 25.9704$$

$$f = \text{fraction of nanotubes that are metallic}$$

$$P_{NC} = \text{probability of a channel that is not connected}$$

$$P_C = \text{probability of a channel that is connected}$$

$$P_M = \text{probability of a channel that is metallic}$$

$$P_{SC} = \text{probability of a channel that is semi-conducting}$$

From optimizing the probability of success in creating a semiconducting channel, three findings are significant:

- The probability of success **decreases** with decreasing channel length.
- The probability of success **increases** with decreasing channel width.
- While the probability of success increases as the channel width decreases, the range of nanotube densities that produce a successful outcome also decreases. The desirable high probability of success has a cost of being very sensitive to density.

Device Characterization

The percolating stick model is a bit over-simplified for characterizing production outcomes. For example, channel could be semiconducting but have an Ion/Ioff ratio that is too low to be considered a successful device. To improve the model, the dispersion is represented as a grid of resistors and nodes. Using Kirchhoff's laws and measured and modeled nanotube conductance and junction conductance, the electronic properties of individual model channels can be estimated. The ensemble statistics of electrical properties of these thin film channels characterizes a production of devices.

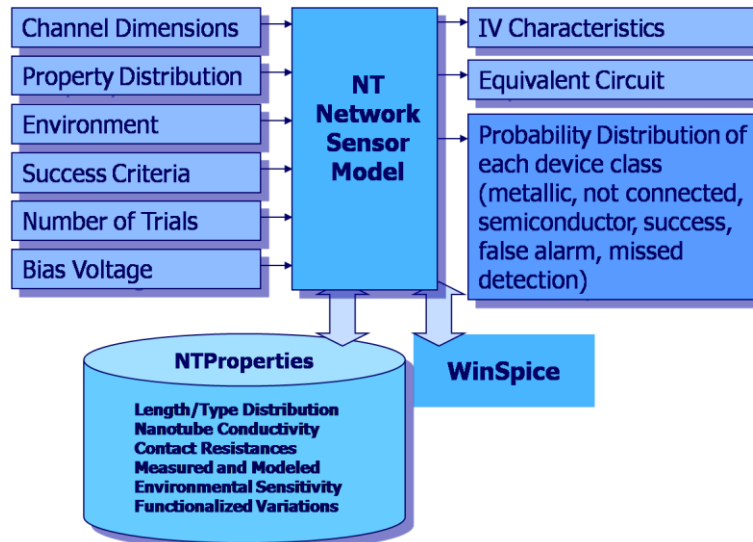


Figure 15: Block Diagram of the Program

A conceptual block diagram of our model is provided in Figure 15. Again, the inputs to the model are the channel dimensions, the fraction of metallic nanotubes, and nanotube density. The bias voltage is another input. As the model runs it accesses a database of nanotube properties. As before, the model outputs the probability distribution functions for each class. Next the locations where nanotubes contact the electrodes and the nanotube junctions in the channel are found. These locations are used to segment the nanotubes into resistors and nodes.

The model also outputs the I-V curve of each device. The table of nodes and resistors is output in a WinSpice format, and a console version of WinSpice is run for different gate voltages. Figure 16 shows a channel, the equivalent circuit, and output I-V curve. The algorithm for modeling a device is to first

populate a channel with nanotubes. Again the location, orientation and classification of each nanotube is maintained in a list.

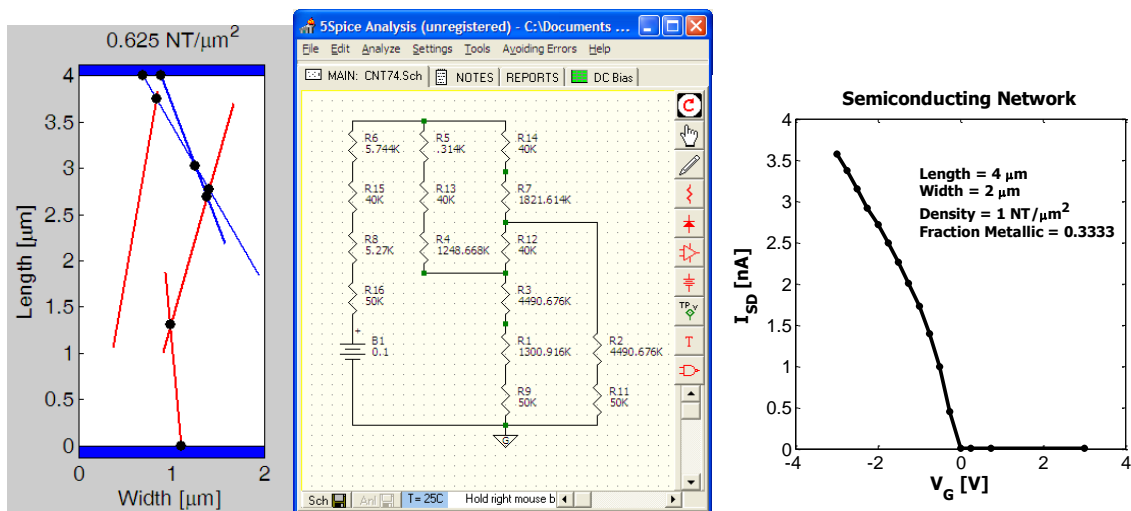


Figure 16: Example of finding the electronic properties of a channel.

This equivalent circuit is analyzed to determine path connectivity and assign a classification: broken, metallic or semiconducting, to the circuit. The electronic properties that are determined by solving the equivalent circuit using WinSpice are then used to determine the I_{on}/I_{off} ratio. Per Kwon, the following logic replaced previous logic for assigning class to a circuit:

1. Success: The device is a semiconductor having a source-drain current $I_{SD} > 10^{-8}$ A and an off current $I_{OFF} < 10^{-10}$ A.
2. Failure: The device is an insulator having $I_{SD} < 10^{-10}$ A.
3. Failure: The device is a conductor having $I_{OFF} > 10^{-10}$ A.

(Note: I didn't know what to do with the devices where 10^{-10} A $< I_{SD} < 10^{-8}$ A and $I_{OFF} < 10^{-10}$ A, but our group was suffering from a lot of turmoil in the months before Kwon announced his eminent departure, and this effort was greatly impacted by that – by not getting direct answers to direct questions.) The outcomes are illustrated in Figure 17.

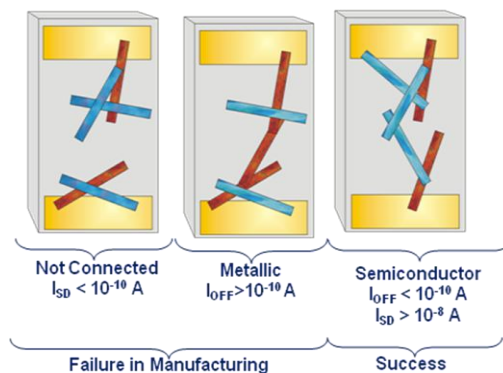


Figure 17: Illustrating the different possible outcomes for channels based on thresholding the off current and the maximum source-drain current.

Performing this sequence many times to acquire statistics for probability distribution functions of each class as a function of density or other manufacturing variable, results in a lot of output that describes each device in the ensemble.

The program is modular and the database is flexible and extensible. Currently, there are nominal properties for nanotube conductivity operating at room temperatures, in ambient environment, and dispersed on a generic substrate. The program is designed to allow that database to grow to include nanotube properties including alternative algorithms for the dispersion statistics, the position and orientation in the channel that simulate bundling or other dynamics; and nanotube properties that are environmentally active to address questions of using the thin film as a sensor and modeling the sensor performance or determining when a device might fail; and compare the performance of different chirality mixtures on different substrates.

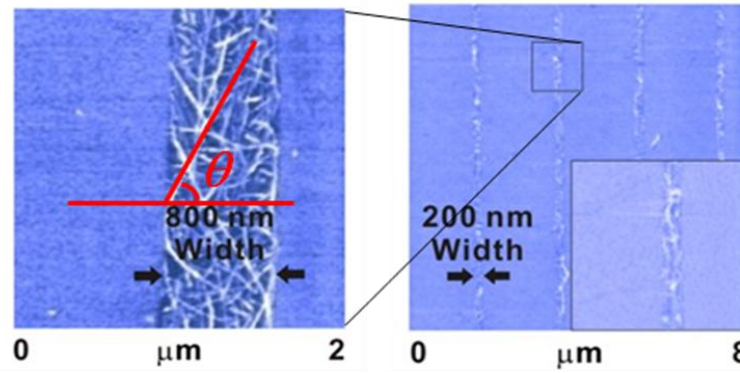


Figure 18: SEM images of an anisotropic channel fabricated by SNU. Here the angle θ is the CW rotation angle of a nanotube the axis along the channel length. Note that while the nanotubes are slightly curved in the fabricated channels, the model regards them as linear sticks. The lengths between junctions are very linear.

Other characterizations output are the anisotropy metric and the effective channel thickness. Balberg, Binenbaum, and Anderson (1983) defined a metric of anisotropy as:

$$Anisotropy = \frac{P_{\parallel}}{P_{\perp}} = \frac{\sum_i |\sin \theta_i|}{\sum_i |\cos \theta_i|}$$

The angle is the clockwise rotation from channel length axis for the nanotube and this is shown in Figure 18. Balberg, Binenbaum, and Anderson only kept networks that had an anisotropy value between 0.95 and 1.05, because they wanted to ensure that their analysis was specific to isotropic stick dispersions. Like the work of Pike and Seager, they were analyzing scaling behavior for infinite systems using novel computational approaches of normalized areas. We also used this anisotropy metric to exclude anisotropic channels from analysis when comparing the scaling behavior for channel length, channel width, and stick length to isotropic percolation models in the literature.

We also defined an effective channel thickness as:

$$t_{\text{eff}} = \frac{V_{NT}}{A_{\text{Channel}}}$$

Where V_{NT} is the to volume of cylindrical nanotubes in the channel, and A_{Channel} is the product of channel length and channel width. SNU measured the effective thickness t_{eff} of the network channels from atomic force microscopy (AFM) topography imaging by dividing the SWNT volume by the pattern area. To have a metric for comparison, this value was also output. (Actually effective thickness, and derivative metrics like conductivity (below), were calculated in a spreadsheet during post-processing analysis, but the intention was to have It in the model.)

The conductivity of the channels was model from the I-V characteristics, effective channel thickness, and channel dimensions:

$$\sigma = \left(\frac{L \cdot I_{SD}}{V_{SD} \cdot W \cdot t} \right)$$

σ = conductivity [S cm⁻¹]
 L = length [micron] (model input)
 W = channel width [micron] (model input)
 V_{SD} = source-drain voltage [V] (model input)
 t = effective channel thickness [cm]
 I_{SD} = source-drain current (computed) [A]

Similarly, the mobility was found from:

$$\mu = \left(\frac{L}{C_0 V_{SD} W} \right) \frac{dI_{SD}}{dV_G}$$

μ = mobility [cm² V⁻¹ s⁻¹]
 L = length [micron] (model input)
 W = channel width [micron] (model input)
 V_{SD} = source-drain voltage [V] (model input)
 C_0 = capacitance per unit
channel area [V C⁻¹ cm⁻²] (fit value of $1.65 \cdot 10^{-8}$ V C⁻¹ cm⁻²)
 I_{SD} = source-drain current (computed) [A]
 V_G = gate voltage [V] (model input)

Characterizing a Mixed Chirality Suspension of Nanotubes

This section provides some of the details about the database of nanotube properties used in the model.

There are two SWNT length distribution functions in the model. The first distribution has an average nanotube length of 3 μm and allows the length to vary up to $\pm 0.3 \mu\text{m}$ using a normal random distribution.

The other is a fit to measured lengths in a SWNT suspension (Figure 19). For the processing done by Dr. Hong's group at SNU is typically 0.1 mg/mL in o-dichlorobenzene. His graduate student Minbaek Lee measured the lengths over 2200 nanotubes and found they had an average length 652.8 nm and a standard deviation of 249.4 nm. The probability distribution is:

$$P(x) = \frac{.57517 \cdot 10^{-15} x^{6.097915}}{e^{0.011120x} - 1}$$

An input to the model is the fraction of metallic nanotubes. A uniform random number is used to set the type of nanotube. Diameter and width of nanotubes are not considered in the model. The model treats all nanotubes as lines. It is assumed that length is independently random of diameter (whether or not the tube is metallic).

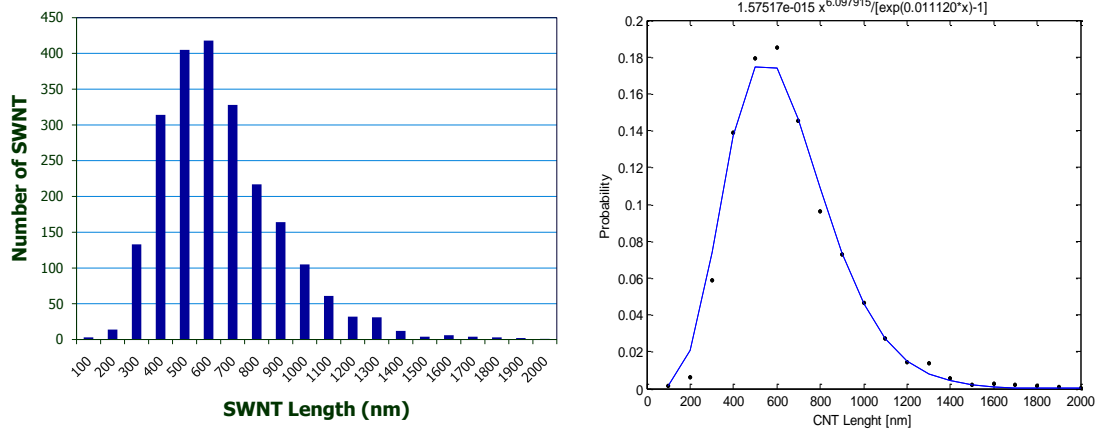


Figure 19: (Left) Histogram of measured SWNT Lengths. (Right) Functional fit to histogram.

The length distribution is used to randomly place and orient a nanotube in the channel. First the length and type (metallic or semiconducting) is randomly assigned; then the center point of the nanotube is randomly assigned with equal probability for all positions in the channel. Once the channel position of the center is known, the range of possible orientations that let the entire nanotube lie inside the channel is calculated. This emulates the lensing effect of SNU's processing for textured networks. The orientation is assigned with equal probability for all angles in that range of possible orientation.

From the type of nanotube, the conductivity and other properties of segments of that tube are determined. Figure 20 shows the two types and their conductivity. The junctions between nanotubes

and between nanotubes are also treated as resistors in the equivalent circuit. Table 3 summarizes these properties.

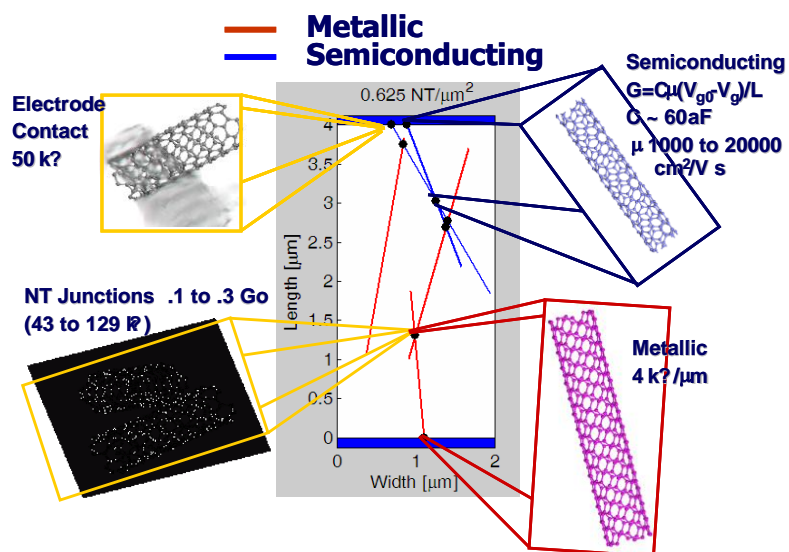


Figure 20: Nanotube properties annotated for a channel.

Table 3: Properties of Individual Single Walled Carbon Nanotubes

Component	Model Value	Reference
NT Length Distribution	Ave=.6 μm	Measurement from Seunghun Hong at Seoul National University, Korea
NT Junctions	40 kΩ	1 to .3 Go (43 to 129 kΩ) Yoon, et. al., Physical Review Letters Vol. 86, No. 4, 2001
Metal/Metal or Semi/Semi	200–400 kΩ	Hecht
Metal/Semi	20000–40000 kΩ	Hecht
NT Contact Electrode	50 kΩ	Kwon
Metallic SWNT	4 kΩ/μm	McEuen, P., MRS Bulletin, April 2004
Semiconducting SWNT	$G = C\mu(V_{g0} - V_g)/L$ $C \sim 60 \text{ aF}$ $\mu \sim 1000 \text{ to } 20000 \text{ cm}^2/\text{V s}$	McEuen, P., MRS Bulletin, April 2004 Burke, PJ IEEE-NANO 2002 Ilani, et. Al, Nature Physics, Vol 2, 2006
Environment Parameters	Semiconducting NT $G = C\mu(V_{g0} - V_g - V_e)/L$ $V_e = f(\text{gas}, P, T, \text{time}, n, m)$ $C_e = f(\text{gas}, P, T, \text{time}, n, m)$	Various experimental & theoretical papers. O2, P.G. Collins, 2000 NH3, NO2 J.Li, 2003 cnt networks NH2-R J.Kong, 2001 HO-R T.Someya, 2003

Model Validation From Scaling Behavior

This section establishes that the model gives expected scaling behavior for ensemble averaged conductivity with nanotube length and with channel length.

Figure 21 and Figure 22 show the comparison of the anisotropic model to the isotropic model of Hecht (2006). It should be noted that when the tubes in the network approach 20–30 microns, the resistance along the tube itself becomes comparable to the resistance of the junction. Although the anisotropic model shows a greater sensitivity of conductivity to nanotube length, both isotropic and anisotropic networks have increased conductivity as the nanotube length is increased. For our simulations the nanotube lengths had a slight variance around the average length for these comparisons.

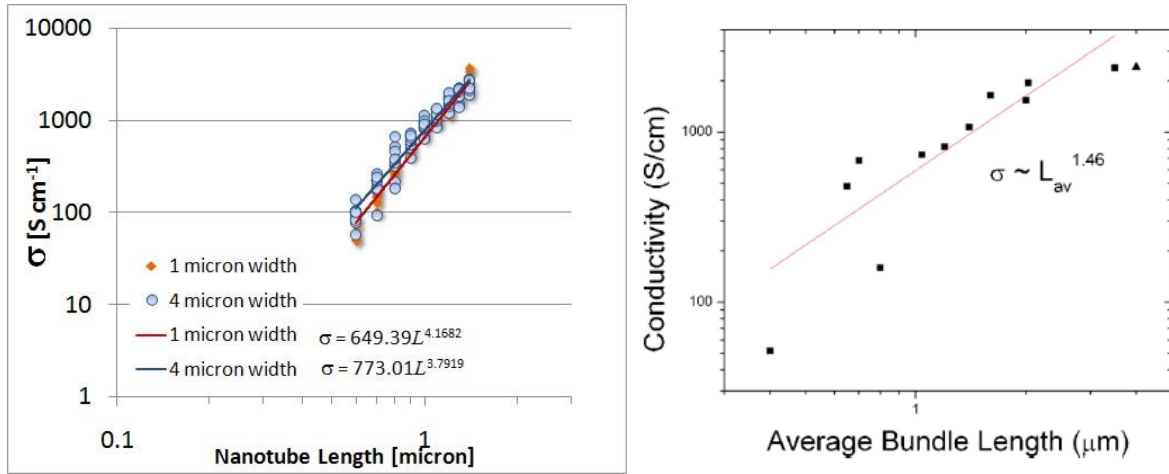


Figure 21: (Left) Model output scaling of conductivity as nanotube length increases. (Right) Conductivity as a function of nanotube length from Hecht, APL, 89, (2006)

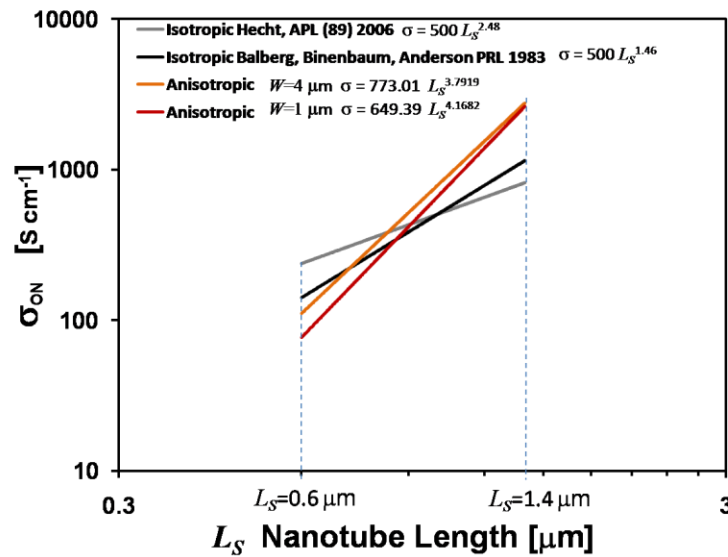


Figure 22: Comparison of scaling coefficients of conductivity as a function of nanotube length for different model output.

Figure 23 and Figure 24 show the scaling behavior of conductivity with channel length for different densities, and further establish the validity of our model.

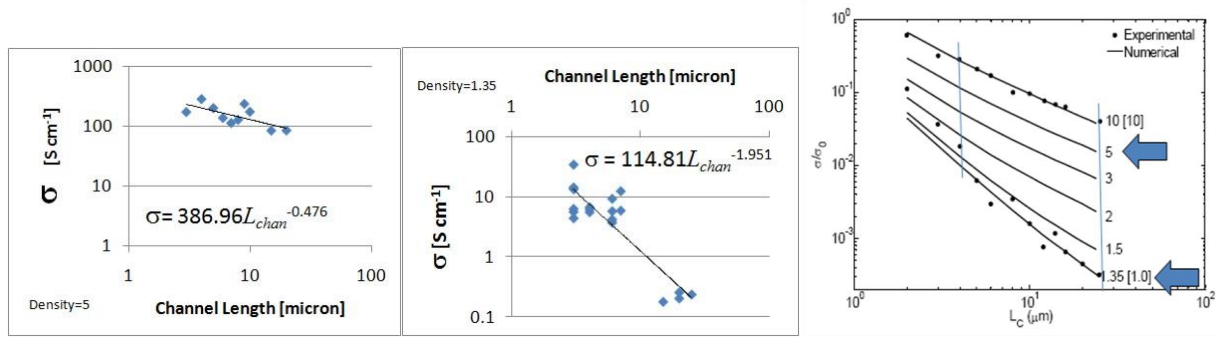


Figure 23: (Top) Two model simulations of the scaling behavior of conductivity at different densities. (Bottom) Experimental and numerical results of an isotropic model published by Pimparkar, Guo, Alam NCN NanoHUB, (2006). The density values corresponding to the anisotropic output are annotated.

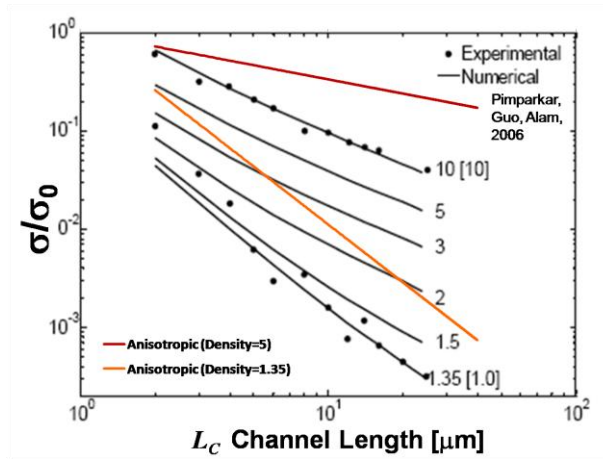


Figure 24: An alternative visualization of the previous results. Here the anisotropic fits are overlaid on the experimental and numerical results of an isotropic model published by Pimparkar, Guo, Alam NCN NanoHUB, (2006).

Comparing the Model To Device Measurements

Minbaek Lee provided device characteristics for low density semiconducting channels and high density metallic channels. Figure 25 shows SEM images of one low density and one high density device. The low density channels were fabricated by first creating patterned substrates dipped in the octadecyltrichlorosilane solution then dipping in SWNT suspension of 0.02 mg/ml for 1 s. The high density channels simply increased the time in the SWNT bath to 60 s.

The model was run for the essentially the same channel dimensions. Per Kwon, our model runs were for devices that are 2 microns in width compared to the fabricated devices that were 2.5 microns in width. Kwon thought that it better represented the degree of anisotropy. An ensemble of devices were modeled, and some I-V curves representing the breadth of output were selected for plotting. The comparison of I-V curves modeled to the measured devices is presented for low density, semiconducting devices, in Figure 26 and for high density, metallic, devices in Figure 27.

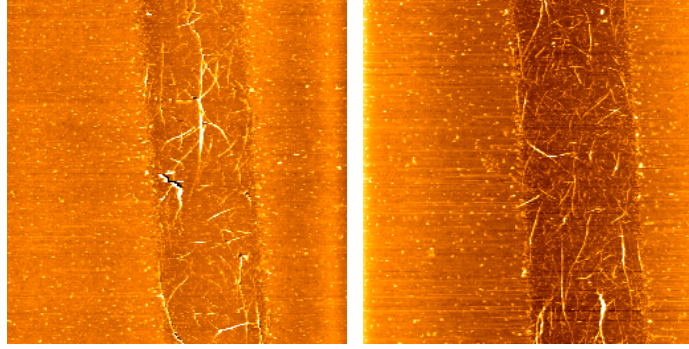


Figure 25: (Left) Low density channel. (Right) High density channel.

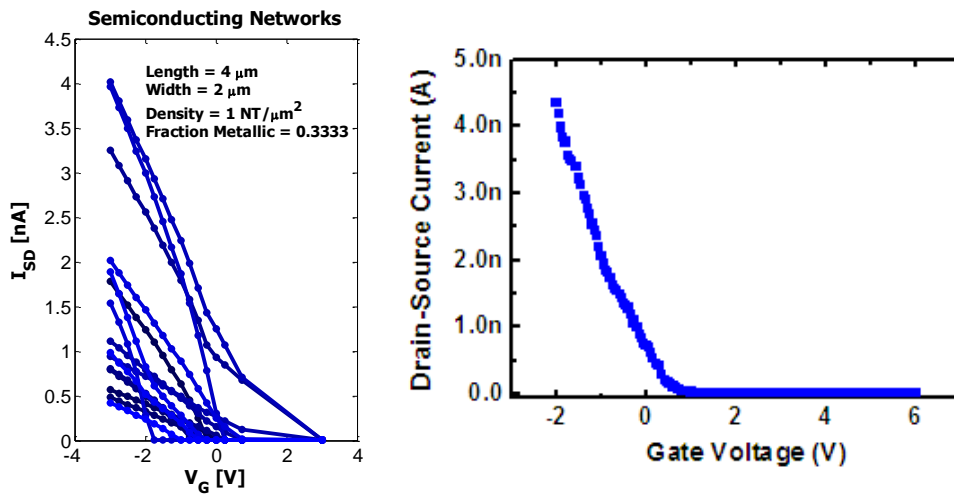


Figure 26: (Left) An ensemble of modeled I-V curves. (Right) SNU measured I-V curve of a single device. In both, the I_{SD} is non zero with $V_G=0$, but a similar range of I_{SD} is found and an $I_{OFF} < 10^{-10}$ A is achieved..

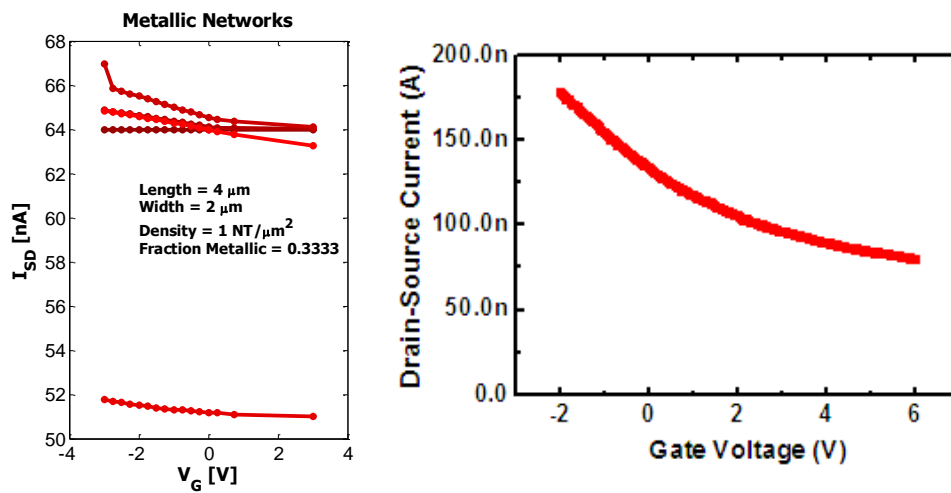


Figure 27: (Left) An ensemble of modeled I-V curves with a density of 1 NT per square micron. (Right) SNU measured I-V curve of a single 'high-density' device. In both, the I_{SD} never off and a similar range of I_{SD} is found.

Comparing the Model To Ensemble Measurements

Minbaek Lee provided ensemble characteristics for a number of different densities to determine the probability of successful outcome for two different channel dimensions: a 20x16 micron channel that is isotropic and a 20x3 micron channel that is anisotropic. The model was run to create ensemble statistics for the same channel dimensions. The model use the nanotube length distribution from SNU's measured values from their vendors suspensions. These are presented in Figure 28, Figure 29, and Figure 30. The results are very comparable and validate that the model predicts the probability of successful manufacturing outcome.

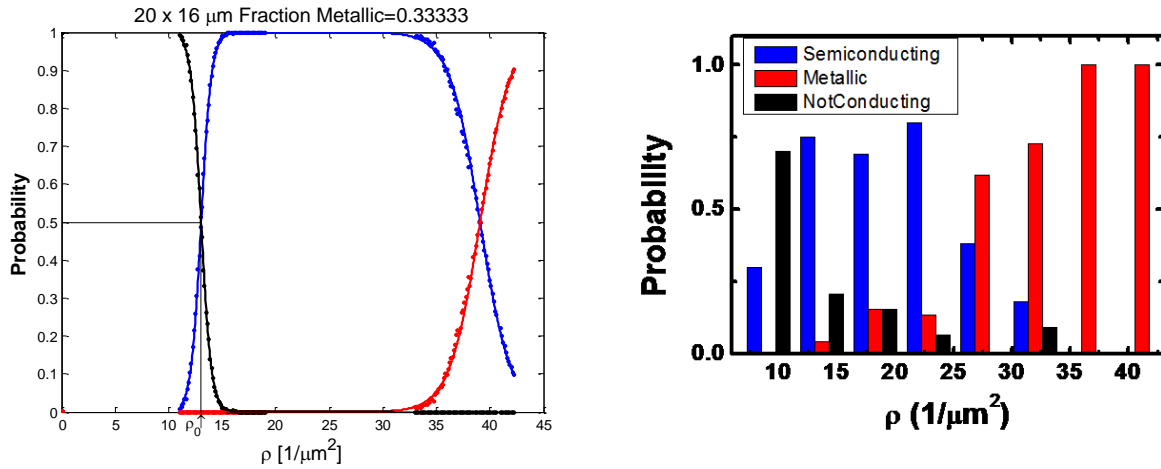


Figure 28: (Left) Model output probability distributions for ensembles with channel length 20 microns and channel width 16 microns. The black lines are not connected or insulating channels. The blue lines are semiconducting channels. The red lines are metallic channels. (Right) Measured ensemble statistics for the same channel dimensions. These channels are isotropic because they are quite wide compared to the nanotube length.

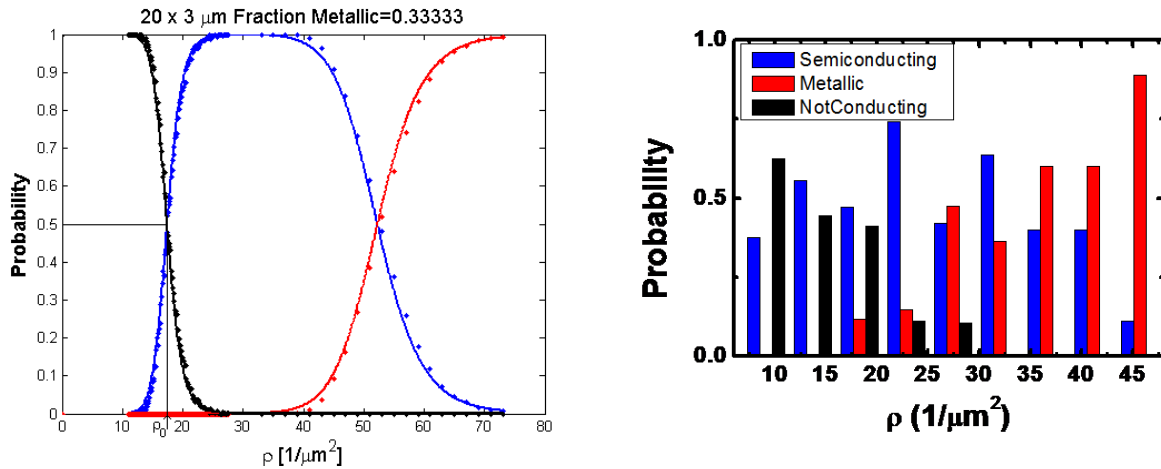


Figure 29: (Left) Model output probability distributions for ensembles with channel length 20 microns and channel width 3 microns. The black lines are not connected or insulating channels. The blue lines are semiconducting channels. The red lines are metallic channels. (Right) Measured ensemble statistics for the same channel dimensions. These channels are anisotropic because they are quite narrow and the orientations are dominated by the lensing effect.

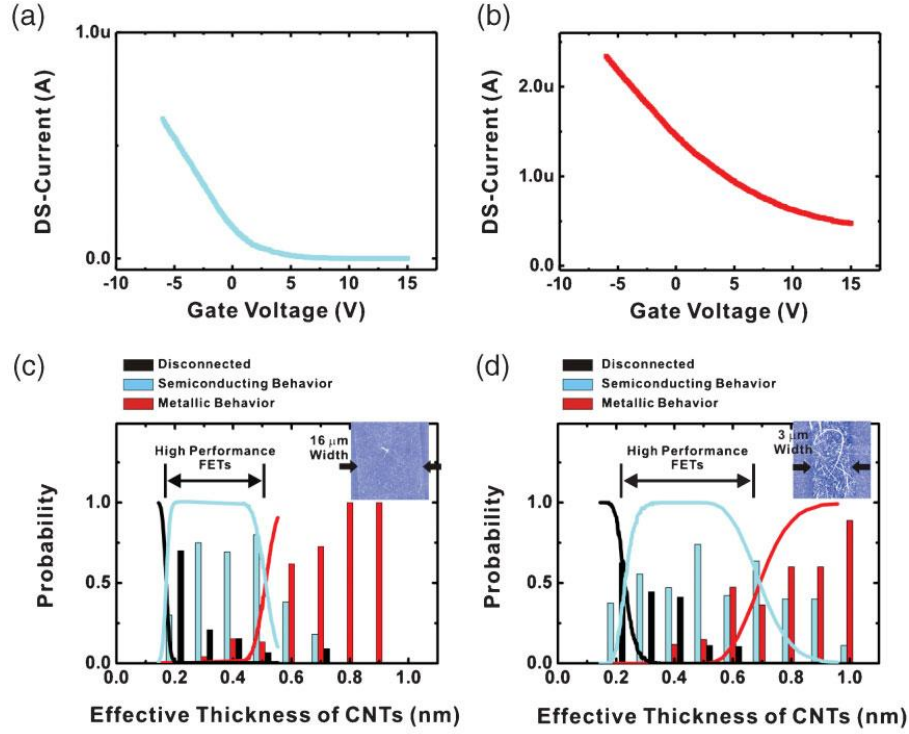


Figure 30: This figure is in the Small (2009) paper and has a different approach to visualization. The caption is: a) A typical gating effect of swCNT network channels with semiconducting behavior. Note that the channel has an off-current smaller than 10^{-10} A. b) A typical gating effect of swCNT network channels with metallic behavior. Note the channel did not turn off even with a large gate bias. c) Distribution of the electric characteristics of 16- μ m-wide and 20-mm-long channels depending on the effective thickness of swCNT network layer. Black, blue, and red blocks represent the probability of having devices with disconnected, semiconducting, and metallic behaviors, respectively. In total, 112 CNT-FETs were tested. The lines represent theoretical simulation results. d) Distribution of the electric characteristics of 3- μ m-wide and 20-mm-long channels depending on the effective thickness of swCNT network layer. Black, blue, and red blocks represent the probability of having devices with disconnected, semiconducting, and metallic behavior, respectively. In total, 120 CNT-FET devices were tested. The lines represent theoretical simulation results.

Next the ensemble electronic properties conductivity and mobility were compared to measured values. The model ensemble averages were made by simulating over 100 devices at each of 5 widths for channels 2 microns long, with the SNU NT length distribution, $V_{SD}=1$ V, and $V_G=-6$ V. The effective thickness was $4.5 \cdot 10^{-8}$ cm, the number of nanotubes for each width was (268, 400, 800, 1600, 3200) for widths (1, 2, 4, 8, 16) microns. The comparisons shown in Figure 31 and Figure 32 have a very good agreement. The log-log plots in the inserts show that the data can be fit well by the curve (red lines) with the scaling behavior of $\sigma_{ON}=w^v$, where $v=0.21$ and 0.19 for modeled and measured respectively. the scaling behavior of $\mu \sim w^v$, where $v=0.21$ and 0.23 for modeled and measured respectively.

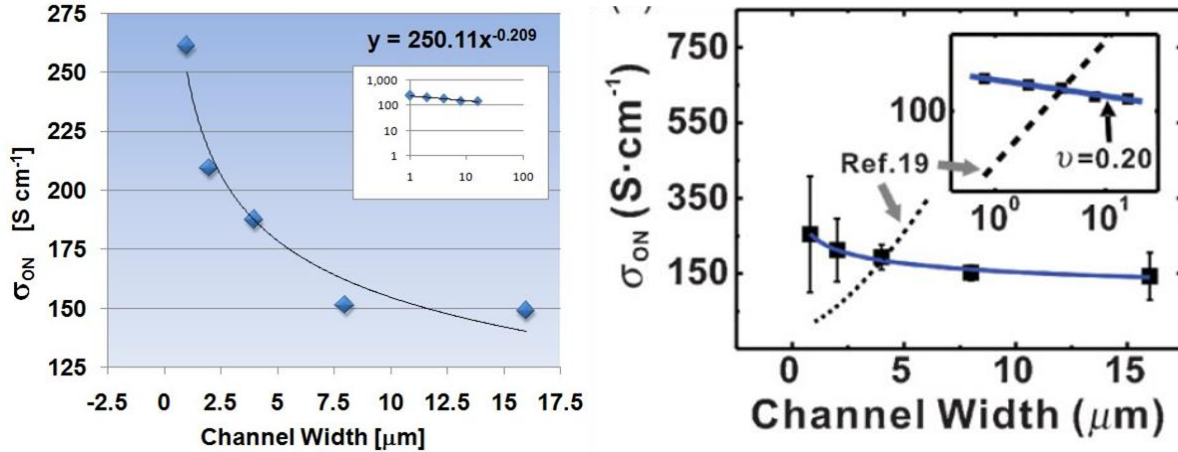


Figure 31: Comparing the scaling behavior of conductivity to measurements. (Left) The ensemble averaged conductivity for model output. (Right) SNU measured conductivity for an ensemble of 100 devices they fabricated.

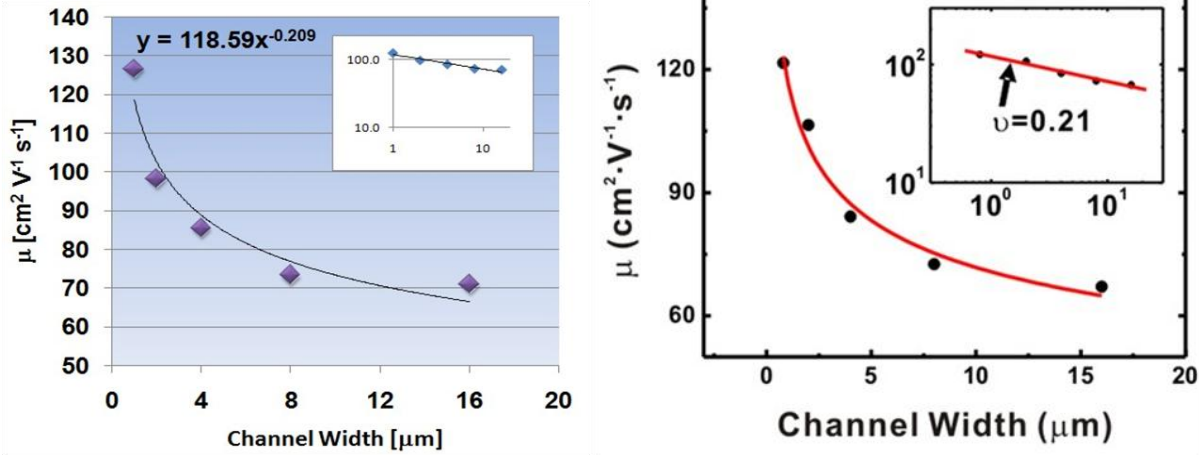


Figure 32: Comparing the scaling behavior of mobility to measurements. (Left) Average mobility for the model ensembles of the previous figure. (Right) SNU measured mobility for their ensemble of 100 devices.

Comparing Isotropic and Anisotropic Scaling with Channel Width

The scaling behavior of conductivity with channel width was validated with measured data. In this section it is compared to the scaling of isotropic models. Previously stated, the take-home message from this research is that although the conductivity of isotropic networks decreases with decreasing channel width as predicted by Benham (2006), it increases with anisotropic networks. Figure 33 and Figure 34 illustrate this in greater detail. Our model can be used to evaluate other performance criteria. For example, in Figure 35 the maximum source drain current is shown to drop with decreasing channel width for anisotropic channels even though the conductivity is increasing.

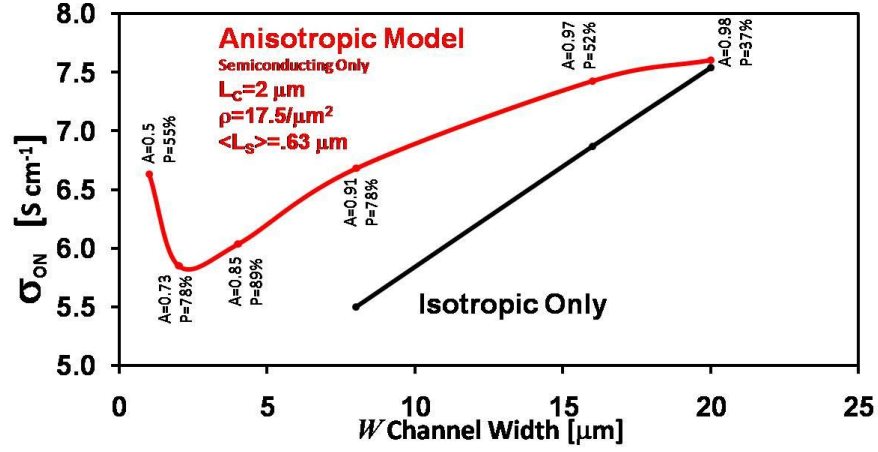


Figure 33: The anisotropic model predicts that conductivity is enhanced when the channel is anisotropic. The red curve is the model output with annotations for the average anisotropy metric at each channel width and with the probability of successfully creating a semiconducting channel. This model output was further analysed to exclude anisotropic channels so that comparison of conductivity from anisotropic to isotropic is made.

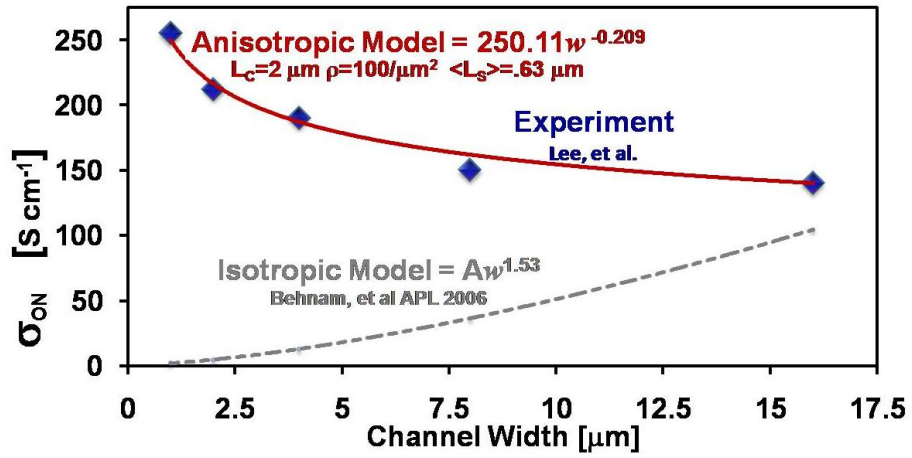


Figure 34: Here the experimental data from SNU and model fit output of the anisotropic model are compared to the isotropic model output predicted by Benham (2006).

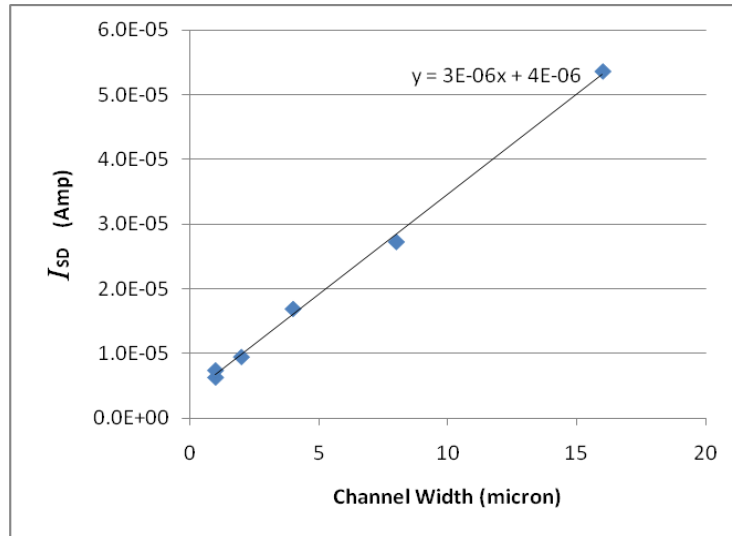


Figure 35: For the conductivity studies, the ensemble averaged maximum ISD does diminish with channel width but not significantly. Here the channel lengths were 2 microns. $V_{SD}=1$ V and $V_G=-6$ V. The effective thickness (a metric now being used instead of density) was 4.5×10^{-8} cm, the number of nanotubes for each width was (268, 400, 800, 1600, 3200) for widths (1, 2, 4, 8, 16) microns. Although this current is dropping, the conductivity is increasing.

Modeling Thin Film Sensors

Thin film nanotube networks have been used for sensors. There are three approaches:

- The nanotubes and nanotube junctions are sensitive to the environment depending on substrate and nanotube type.
- Nanotubes can be functionalized to selectively adsorb specific molecules.
- SNU's approach is to functionalize via the patterning. So different patterns might cause nanotube arrays to selectively adsorb specific molecules. Figure 36 shows their concept.

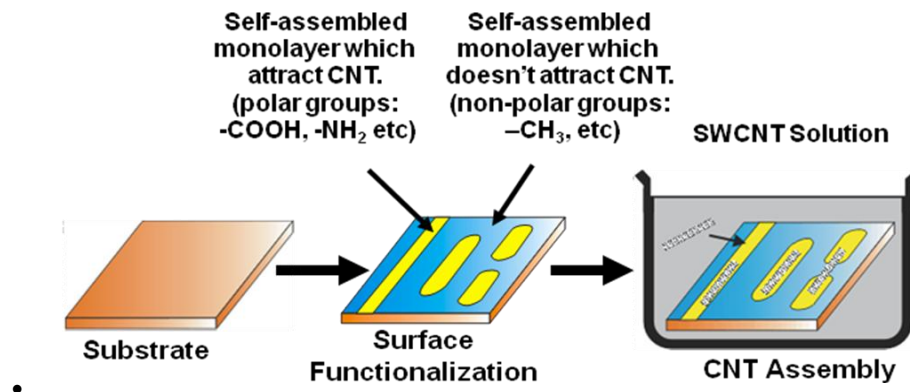


Figure 36: The surface patterning can be used to create a functionalization of the arrays.

For simple networks, environmental sensitivity of exposure to gases, fluids, contact forces, and temperatures have been suggested for sensor design. For carbon nanotubes, NH_3 is an electron donor, and NO_2 , CH_4 , H_2 , O_2 , and CO_2 donate holes. These charge transfers change the device characteristics.

In fluids like acetone or saline water, the nanotube electronic properties change. The resistances of nanotube junctions are sensitive to contact forces.

For a sensor model, new classifications of outcome are needed (Figure 37):

- Success: Detected environmental factor of interest.
- Failure: False positive because a different substance was misidentified.
- Failure: False positive because the quantity was insufficient to trigger alarm.
- Failure: Missed detection.

Additionally, performance metrics regarding sensitivity, stability, and selectivity are needed. Sensor suites can be fabricated to allow selective strategies. For example, multiple channels with different responses to same gas used to logically with voting schemes, or to enable a greater dynamic Range and sensitivity for measuring concentrations, forces, and temperatures, to improved sampling, and for evaluating the dynamic flow past multiple test positions.

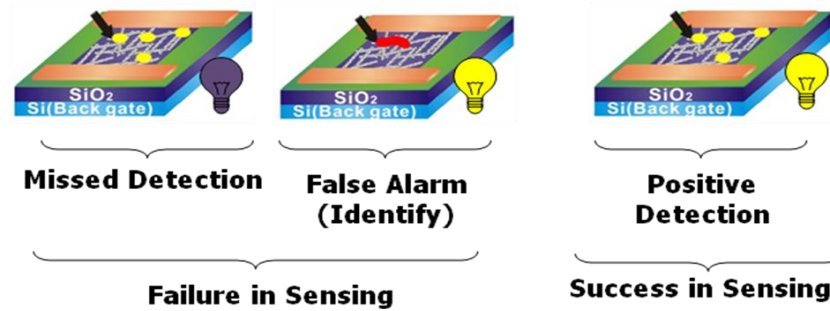


Figure 37: Classification in the Probability of Success for a Sensor.

As a proof-of-concept, the model was extended to show the difference in I-V characteristics when the array was saturated with NO₂. Figure 38 shows that detection is possible for this situation, and the detectability changes with different nanotube densities. Here the channel length is 4 microns, the channel width is 1 micron and is populated with the SNU distribution of nanotube lengths with 1/3 being metallic. Even the metallic channels show theoretical potential for being an environmental sensor.

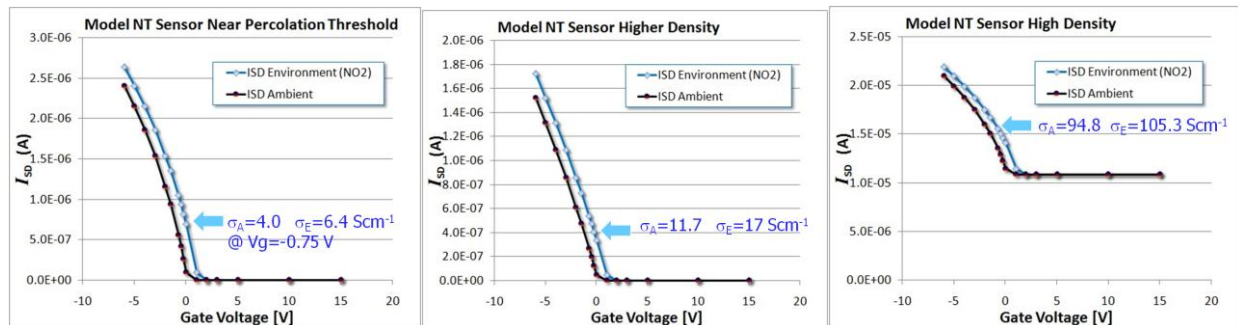


Figure 38: Even at high densities, where the channels are metallic, the thin film networks theoretically perform as environmental sensors.

Conclusions

Thin films of single walled carbon nanotubes (SWNTs) are a new class of transistors, one of the current leading technologies to replace MOSFET devices. Recent developments in creating thin film SWNT networks allow the production of anisotropic or 'textured' networks that exhibit enhanced electronic properties. New models, however, are needed in order to design circuits using these methods. We have developed a first principles percolating stick model to predict properties of ensembles of networks using Monte Carlo simulations. This model enables understanding of both the scaling behavior of the degree of anisotropy in a channel and the electronic properties of a channel as a function of the degree of anisotropy.

The significance of our work is that this model enables design of nanoscaled electronic circuitry. While traditional isotropic models predict that conductivity as $\sigma \sim w^{1.53}$ for short channel widths, w , our results show that conductivity of anisotropic channels increases with decreasing width as $\sigma \sim w^{-0.2}$.

Our results:

- Explain why measurements of textured networks show improved conductivity with narrow channels.
- Show that traditional percolation models are insufficient for textured networks.
- Characterize nanotube network ensembles.
- Model the network I-V curves, conductivity, and mobility in different environments.

Our work has been published in peer reviewed journals.

Future Work

With Dr. Kwon's departure, the opportunity for future work in developing the model is no longer available. But our plans were to expand database of nanotube parameters to consider dispersions with bundling, investigate performance dependence on substrate, and understand the influence of a variety of environmental factors. We had intended to model ensemble statistics of I-V curves and values quantifying production parameters in terms of mobility, dynamic range, etc. There are more percolation models to compare our model to, and additional verification and validation with experimental data is needed to develop a robust model. Our methodology would have been expanded to include ab initio density functional theory computations for defect analysis. To that end, density functional theory was used to investigate adsorption forces between different industrial compounds and nanotubes and substrates, and Al₂O₃ was studied and according to literature is a potential substance to coat sensors with to enhance design life and durability.

References

Behnam, A., L. Noriega, Y. Choi, Z. Wu, A. G. Rinzler, and A. Ural, Appl. Phys. Lett. 89, 093107 (2006)

Frank, Stefan, et. al, Science, 280 (1998)

Snow, E. S., P. M. Campbell, M. G. Ancona, and J. P. Novak, APL, 86, 033105, 2005

Sanvito, Stefano, Young-Kyun Kwon, David Tomanek, and Colin Lambert, PRL, 82 (2000)

Thess, Andreas, Roland Lee, Pavel Nikolaev, Hongjie Dai, Pierre Petit, Jerome Robert, Chunhui Zu, Young Hee Lee, Seong Gon Kim, Andrew G. Rinzler, Daniel T. Colbert, Gustavo Scuseria, David Tomanek, John E. Fischer, Richard E. Smalley, Science 273, 483 (1996)

McEuen, P. and Ji-Yong Park, MRS Bulletin, (2004)

Burke, PJ IEEE-NANO (2002)

Ilani, et. al, 'Measurement, Nature Physics, Vol 2, (2006)

Yoon, et. al., PRL, 86, (2001)